The influence of feedback and convection on imposed heating conditions when using gas-fired radiant panels in fire testing

Citation for published version:
Cadosch, H, Morrisset, D, Law, A, Terrasi, G & Bisby, LA 2023, 'The influence of feedback and convection on imposed heating conditions when using gas-fired radiant panels in fire testing', *Fire Safety Journal*, vol. 141, 104013. https://doi.org/10.1016/j.firesaf.2023.104013

Digital Object Identifier (DOI):
10.1016/j.firesaf.2023.104013

Link:
Link to publication record in Edinburgh Research Explorer

Document Version:
Peer reviewed version

Published In:
Fire Safety Journal

The influence of feedback and convection on imposed heating conditions when using gas-fired radiant panels in fire testing

Hussein Cadosch[a,b*], David Morrisset [a], Angus Law [a], Giovanni Terrasi [b], Luke Bisby [a]

[a] School of Engineering, The University of Edinburgh, UK, hussein.cadosch@ed.ac.uk

[b] Empa, Swiss Federal Laboratories for Materials Science and Technology, Switzerland

*Corresponding author

Highlights:

- Quantification of convective influence zone for gas-fired radiant panel arrays.
- Quantification of thermal feedback effects on the presumed boundary conditions.
- Suggestion of a correction method for thermal feedback effects.

Abstract:

Gas-fired radiant panel arrays (RPAs) are a common experimental tool used in fire science and material testing. Unlike devices such as Cone Calorimeter or the Fire Propagation Apparatus (FPA), RPAs typically consume gaseous fuel within a porous medium through which fuel is burnt. When RPAs are used, thermal feedback from the surface of heated samples, as well as the effects of hot gases within the zone of convective influence of the RPA will cause an increase in the surface temperature of the RPA. To investigate this, experiments were conducted using a gas-fired RPA. Target samples made from vermiculite board, concrete, and a water-cooled aluminium plate were exposed to various severities of pre-calibrated incident radiant heat fluxes (HF). It was confirmed that the presence of a target sample led to an increased surface temperature for the RPA of nearly 80 °C (for a calibrated incident HF of 144 kW/m^2). This increased surface temperature results in an incident HF nearly 78% higher than the pre-calibrated value at the sample's surface. Based on the results in this paper, a correction method has been proposed which can be used by gas-fired RPA users to account for the increase in incident heat fluxes.

Keywords: heat transfer; radiant panel arrays; thermal environment; thermal feedback; incident heat flux.

1. Introduction

Externally applied radiant heat fluxes (HF) are a common thermal boundary condition used in the field of fire science, for both standard tests and exploratory experiments. Various instruments may be used to generate radiant HF, including electrical coils in the Cone Calorimeter [1], lamps in the Fire Propagation Apparatus (FPA)[2], and gas-fired radiant panel arrays (RPAs) in e.g. the "H-TRIS" methodology [3]. The latter generally comprises a porous medium in which a mix of gas and air are burned at a constant rate so to maintain a constant temperature at the panel surface. When choosing appropriate equipment for testing, RPAs have advantages in robustness, scalability, and the ability to produce comparatively high heat fluxes (panel temperature can exceed 1200 °C for some systems). Further, the modularity of RPAs makes them adaptable (compared to the cone calorimeter or FPA) should users want to investigate new configurations or larger scales. Users of gas-fired RPAs have utilised them to experiment on a range of varied materials and using different thermal boundary conditions [4]–[13].

The coil of the cone calorimeter and lamps of the FPA control the power of the apparatus by varying the temperature of the radiating element (i.e., the cone or bulb temperature). The relationship between element temperature and HF is then used to regulate the HF exposure of the test sample. Conversely, gas-fired RPAs are typically operated so as to produce a constant temperature as a result of the combustion taking place within the porous matrix; as such, the desired incident HF to which a target sample is subjected is varied by changing the separation distance between the RPA and the target sample (and hence the view factor for radiation). Experiments requiring high heat fluxes use smaller separation distances between the RPA and the target sample compared with experiments that require lower heat fluxes. For the highest incident heat fluxes – and hence the lowest separation distances – it is possible for the target sample to be located *within* the plume generated by the RPA. The interaction of these hot gases with the target therefore increases the complexity of the thermal exposure. The target is subject to both an external radiant flux, and a convective boundary condition associated with the flow of hot gases. The plume generated in front of the RPA may be affected by the pressure drop across the RPA mesh, however this is would not be causing variations from one set of experiment to the next one.

A recent preliminary study by the authors also demonstrated that the potential for a non-negligible radiative feedback between the target sample and the RPA – causing an increase in the panel surface temperature [14] particularly at smaller separation distances between the RPA and the target samples. This feedback has the potential to invalidate the fundamental assumption of constant panel temperature throughout the duration of an experiment. These two considerations (convective influence from the plume, and radiation feedback from the sample to the RPA) are likely to impact on the accuracy and validity of any experiments using an RPA for a calibrated, radiant heat flux. Understanding these effects and accounting for them is therefore important for those wishing to obtain reliable, quantified data from experiments with RPAs. This paper sets out a systematic investigation of the effects of the testing environment on the thermal boundary conditions imposed on potential target samples under a range of relevant conditions.

2. **Methodology**

To investigate the extents of the zone of convective influence and the magnitude of the effects of radiation feedback from the sample to the panel, a mobile RPA (also known within the community as H-TRIS) at the University of Edinburgh was used [15]. The specific RPA used in this study comprises four burners that reach a temperature of approximately 1200 °C under normal (free space) operating conditions. After ignition of the panels, the flow of gas to the porous medium is stabilised at approximately 1.25 grams per second, and electrical fans are used to pre-mix the fuel with air in optimised proportions before entering the combustion media. The gas used is commercially available propane, while the air supply to the panels is 60 g/s as specified by the panel manufacturers.

2.1. Location of hot gases

To detect the extent of the zone of convective influence, gas phase thermocouple measurements were made at various separation distances from the RPA and at various heights. Two sets of measurements were made, one with a small vermiculite heat barrier (50 mm × 50 mm) between the thermocouple and the RPA, and one without. The intent of the heat barrier was to block direct radiation from the RPA – and therefore allow the location at which there was an onset of convective influence to be identified. This concept has been shown graphically in Figure 1. Further measurements were made using a 0.5 mm Inconel sheathed Type K thermocouple (TC) at nine separation distances from the RPA surface, namely 50, 75, 100, 125, 150, 200, 300, 400, and 500 mm. This process was repeated at various points across the surface of the RPA. Additional details of the approach used are reported in [14]. Once these data were gathered, the boundary of the zone of convective influence was (semi-arbitrarily) defined using the criterion given in Equation 1:

$$(T_{surf} - T_{measured})/(T_{surf} - T_{ambient}) = 0.9. \quad (1)$$

Where T_{surf} is the surface temperature of the RPA, measured directly using 4 thermocouples that were placed within the porous medium, $T_{measured}$ is the measured gas-phase temperature, and $T_{ambient}$ is the ambient temperature.

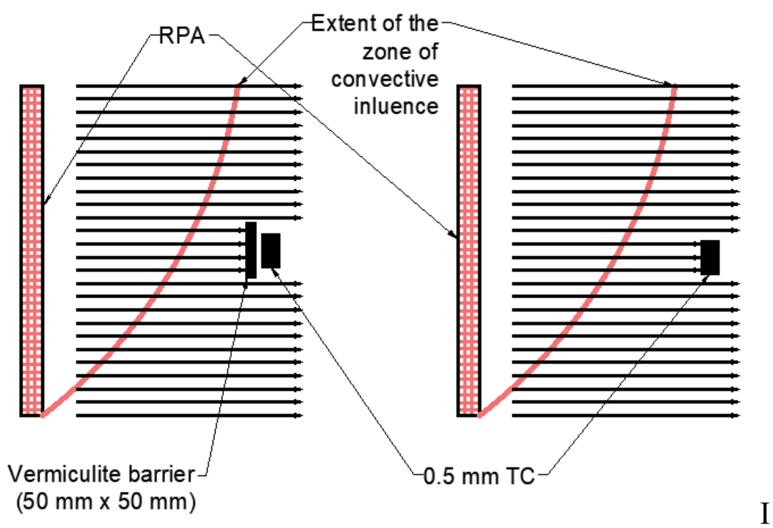

Figure 1 A schematic showing the set up used to establish the extent of the zone of convective influence. In the first case (left), a small vermiculite barrier prevents radiation from reaching the TC, while the TC is fully exposed to oncoming radiation from the RPA in the second scenario (right).

2.2. Feedback to panels

To establish the degree to which radiant feedback to the panels from the sample might influence the RPA temperature and hence the imposed incident heat flux, a series of experiments was carried out with four different targets with varying thermal inertia. The intent was that each of these target surfaces would have different time-histories of surface temperature under a given calibrated incident HF exposure, and would thus produce different heat feedback to the panels of the RPA.

The first configuration was representative of the configuration that is typically used to calibrate gas-fired RPAs. That is, a free floating, water-cooled HF gauge (see Figure 2) was used, without any surrounding sample. The HF gauge was manufactured by Hukseflux, with a rated measurement range of 250 kW/m^2 and a calibration uncertainty of ±0.006 × 10^{-6} V/(W/m). Two additional configurations corresponded to target specimens that were representative of commonly tested materials were also tried. Specimens of concrete and vermiculite board of plan dimensions 400×300 mm were placed in front of the RPA. The HF gauge was embedded in the sample in such a way that the gauge was flush with the surface of the target sample (see Figure 2). This approach allowed the differences due to the presence of a heated target sample to be quantified. For these experiments, the sides of the (water-cooled) HF gauge were insulated from the walls of the target sample using two layers of ceramic paper.

The final experimental configuration used a water-cooled aluminium plate (again 300×400 mm in plan dimensions). The objective was to eliminate significant temperature increase at the target surface – thereby eliminating any radiant feedback from the specimen to the RPA. The water-cooled plate was fabricated using aluminium hollow sections (with a wall thickness of 6 mm) that were welded together; this allowed for an even flow of high volume of water through the plate. The plate was coated with a highly emissive matt black paint to mitigate reflection to the RPA. A 50 mm diameter hole was also fabricated into the centre of the water-cooled aluminium plate to enable an HF gauge to be placed in that location during the experiments (see Figure 2). The water-cooled plate was painted matt black. The surface temperature of the water-cooled aluminium plate was monitored using two Type K TCs that were welded to its exposed surface. The water flow through the water-cooled plate during the experiment was 0.185 litres/second.

Figure 2 shows the various HF gauge arrangements used in this study. For each scenario, incident HF was measured at separation distances of 100, 125, 150, 200, 300, 400, 500, 750 and 1000 mm. In addition to recording the incident heat flux, the temperature of the RPA was monitored using four Inconel-sheathed Type K TCs that were placed within the porous medium of the panels. The intent of this was to allow for any changes in temperature of the panels to be measured directly (as well as indirectly via radiation measurements from the HF gauge). Measurements from the type K TCs were verified using a platinum TC with a maximum operating temperature of 1500 °C.

All heat flux measurements were averaged over a 1 min period, over which the heat flux reading fluctuated by no more than 2 kW/m^2. The time to reach a steady heat flux value was material dependent; concrete, for example, required upwards of 10 min to reach a steady condition due to the high thermal inertia and delayed heating of the solid compared to vermiculite which stabilized in approximately 2 min or less.

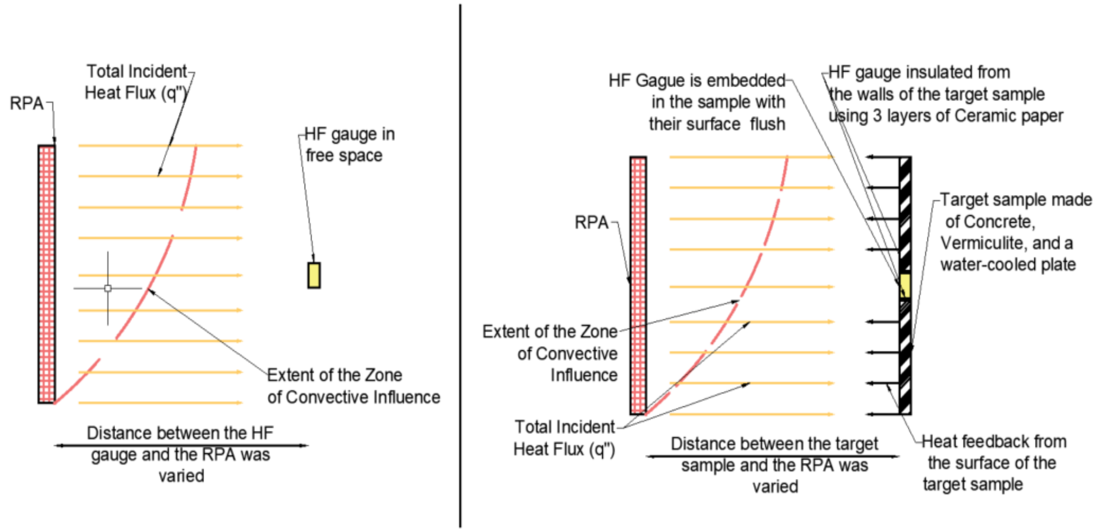

Figure 2 Diagrams showing the set-up used for to measure feedback. On the left, the HF gauge is situated in free space (No Sample), while on the right, the HF gauge is embedded in a target sample and a restraining frame faced with vermiculite boards that are flush with its surface (Concrete, Vermiculite, and Water-cooled plate samples).

A vermiculite protection board (with a window in the middle for the samples) was used for all the cases except when measurement was being recorded for the no sample case. The vermiculite shield was used to protect the instrumentations behind it from exposure to heat (see Figure 3).

Figure 3 An example of the set up used to measure the heat feedback from the target samples to the RPA. The vermiculite shield can be seen in the picture too.

3. Results and discussion

3.1. Zone of convective influence

As stated in Section 2.1, the onset of the zone of convective influence (i.e., the extent of the plume of hot gas generated by the RPA) was determined by employing a TC with and without a 50 mm × 50 mm vermiculite radiation barrier (see Figure 1). Figure 4 demonstrates the efficacy of the radiation shield up to a separation distance of 200 mm. When the separation distance was reduced to 150 mm, both sets of measurements exhibited similar results, confirming the TC's placement within the zone of convective influence. The extent of the zone of convective influence was (more accurately) determined through unshielded gas phase thermocouple data and Equation (1). With the surface temperature of the RPA measured at 1200 °C and assumed to remain constant in these trials, and taking the ambient temperature to be 25 °C, Equation (1) was used to produce Figure 5; The zone of convective influence defined in this way extended to a maximum of 192 mm from the surface of the RPA. Thus, any target sample less than approximately 200 mm away from the surface of the RPA is thus likely to be significantly influenced by the zone of convective influence. Figure 5 (solid black line) shows the extent of the zone of convective influence defined in this way at various points over the height of the RPA (with the face of the RPA located at zero on the x-axis). Figure 5 also shows the temperatures measured in the gas phase (unshielded); these measurements were taken the points shown in red dots.

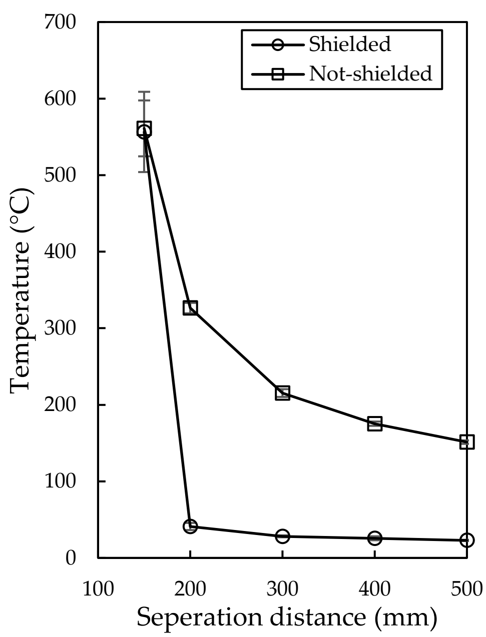

Figure 4 Measured temperature using a 0.5 mm TC with and without the use of a 50 mm^2 vermiculite barrier.

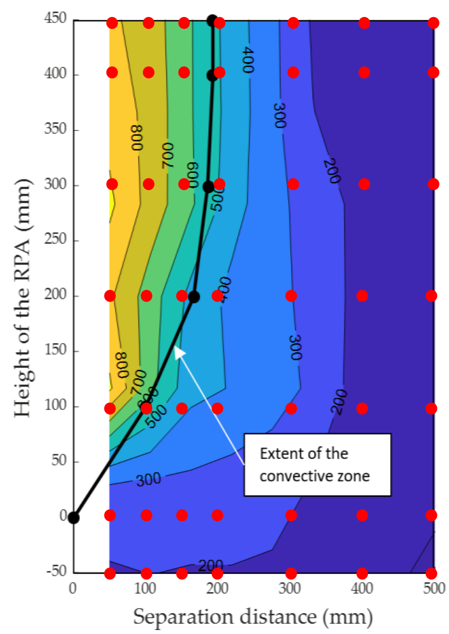

Figure 5 Gas phase temperature profiles obtained using unshielded TCs (grid shown in red dots). The extent of the zone of convective influence defined as discussed is also shown.

3.2. Heat flux measurements

The results of the HF measurements using an HF gauge in isolation is shown in Figure 6. A comparison between the measured values of incident HF perpendicular to the centre of the RPA (at given separation distances) and calculated values of the incident HF at the same positions is also shown in Figure 6. The calculated values are derived based on the view factor method outlined in [16]. The surface temperature of the RPA was measured as approximately 1200 °C (±21), and an emissivity of (0.78) was utilised, which was obtained from [17]. Figure 6 shows that the initial calculated HF (up to a separation distance of 200 mm) accords well with the measured values for the same separation distance (approximately 2 kW/m^2, or 7% difference at a separation distance of 500 mm).

However, for separation distances of 200 mm or less, the measured values of the incident HF were found to be larger than the calculated incident HF; when the distance between the HF gauge and the RPA was 100 mm, the measured incident HF was nearly 21% higher (25 kW/m^2 higher) than the estimated incident HF value. With reference to Figure 2, this discrepancy is likely the result of the HF gauge being within the plume of the RPA (i.e., the zone of convective influence), since the zone of the convective influence of the RPA extends to nearly 200 mm from the surface of the RPA at the RPA mid-height. This effect is similar to what has been reported for the cone calorimeter [18], where the fraction of the heating flux accounted for by convection was in the region of 8-12%, although the convective zone in the Cone Calorimeter, unlike in the RPA, is the result of natural convection alone. It is assumed that the larger fraction observed for the RPA (compared to the Cone Calorimeter) was due to the forced flow of air required to maintain the combustion taking place within the porous medium of the RPA, compared to the natural convection of the cone.

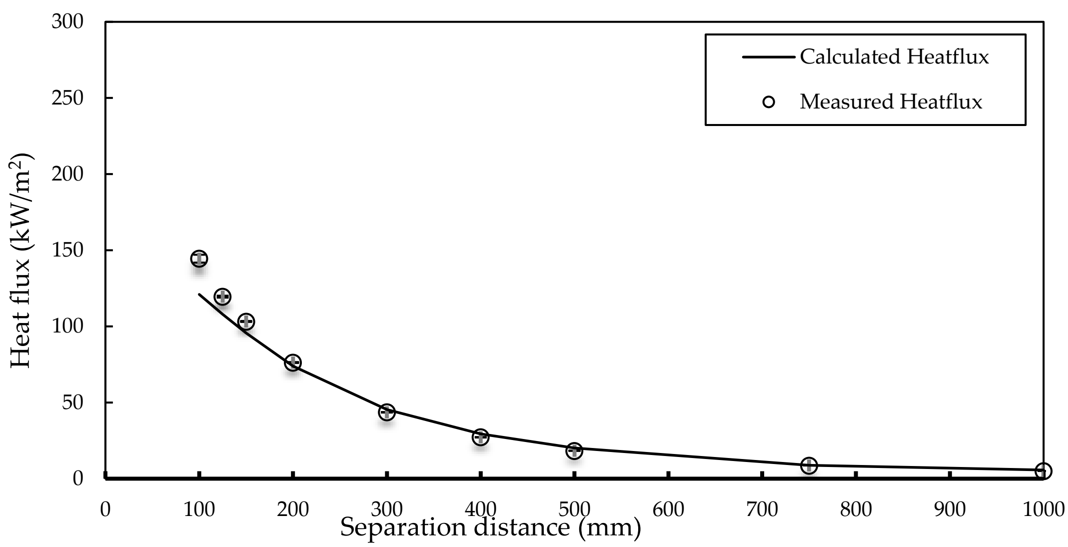

Figure 6 Calculated incident HF compared to that measured with a water-cooled HF gauge at the centre of the RPA (as a function of separation distance from the surface of the RPA)

Close proximity between the RPA and the HF gauge (i.e. proximity where the above influences can become important) is a common when employing gas-fired RPAs for experiments that require heat fluxes in excess of 80-100 kW/m^2 [19].

3.3. Sample Heat Feedback

Figure 7 shows the results of the measured incident HF both with and without the presence of a target sample (vermiculite, concrete, and water-cooled plate samples). As already mentioned, the HF gauge was embedded in the centre of the target sample, flush with its surface. The results show that the presence of a sample increased the incident heat flux measured; when a concrete sample was used, the HF (for a separation distance of 100 mm) was nearly 57% higher (227 kW/m^2) than when no sample was present (144 kW/m^2). The difference in the measured HF was 78% (for the same separation distance) when a vermiculite sample was used (256 kW/m^2). Figure 7 also shows that the difference in the incident HF between the various arrangements was negligible when the separation distance was 500 mm or more. The variation between the increased incident HF for concrete and vermiculite samples only appears when the separation distance is about 150 mm or less. This could be explained by thermal response of the samples to the heat exposure; the vermiculite sample had a thickness of only 25 mm while the concrete sample had a thickness of 50 mm. This caused the vermiculite sample to thermally bow towards the RPA more than the concrete sample (which was restrained more by its colder regions). This means that the vermiculite sample was effectively closer to the RPA surface than the concrete sample was at high heat fluxes. This observation was visually estimated (as opposed to measured) to be in the order of 10-15 mm. Nonetheless, the difference mentioned falls within the margins of the gauge uncertainty for such high heat fluxes, as shown in Figure 7.

For the cases where a heated sample was used, the increase in the measured values of the incident HF was explained by the heat feedback (through radiation) from the surface of the heated samples, and through convection from the zone of convective influence. The heat feedback leads to an increase in the surface temperature of the RPA, which leads to a higher incident HF. The increased surface temperature of the RPA has been shown in Figure 8. This phenomenon has been accounted for in devices such as the cone calorimeter where a series of TCs record the surface temperature of the coil and the power input is manipulated to maintain a constant surface temperature [20]. Given that the gas and air flow into the RPA is kept constant, a rise in the surface temperature of an RPA is inevitable (provided no mitigating action is taken) once a heated target sample is placed in front of it.

Figure 7 also shows the measured HF when a water-cooled plate was used. The measured HF for the water-cooled sample was recorded to be bigger than the HF values for the no sample case (17% at a separation distance of 100 mm). The difference between the HF values for the water-cooled sample and the no sample case can be seen to appear once the separation distance is 300 mm or less.

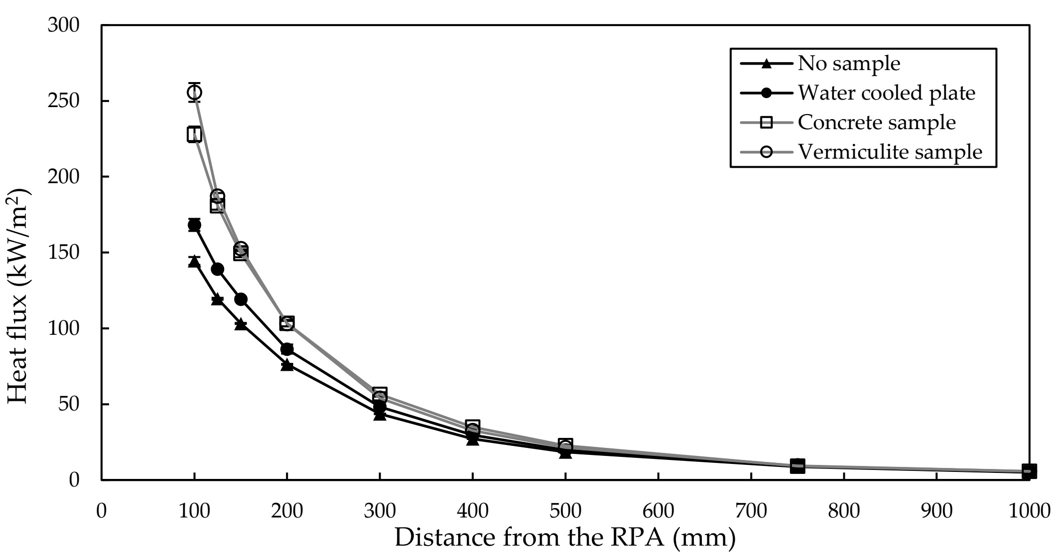

Figure 7 Measured incident HF at the centre of the RPA with and without the presence of a target sample. Results for both vermiculite and concrete target samples shown.

The higher HF values for the water-cooled sample compared to the no sample case could be explained by the small increase in the RPA surface temperature due to the heat feedback from the vermiculite shield used (see Figure 3).

The increased surface temperature of the RPA was thus observed to depend significantly on the nature (i.e. heating) of the target sample; for a vermiculite target sample, the increase in the surface temperature of the RPA was recorded to reach nearly 80 °C at a separation distance of 100 mm, while an increase of only 14 °C was measured the same separation distance when a water-cooled plate was used. The rise in the surface temperature of the RPA is shown as a function of the separation distance between the RPA and the target sample in Figure 8. The rise in the surface temperature of the RPA would be originating from the heated target samples, as well as a small contribution from the vermiculite shield (see Figure 3).

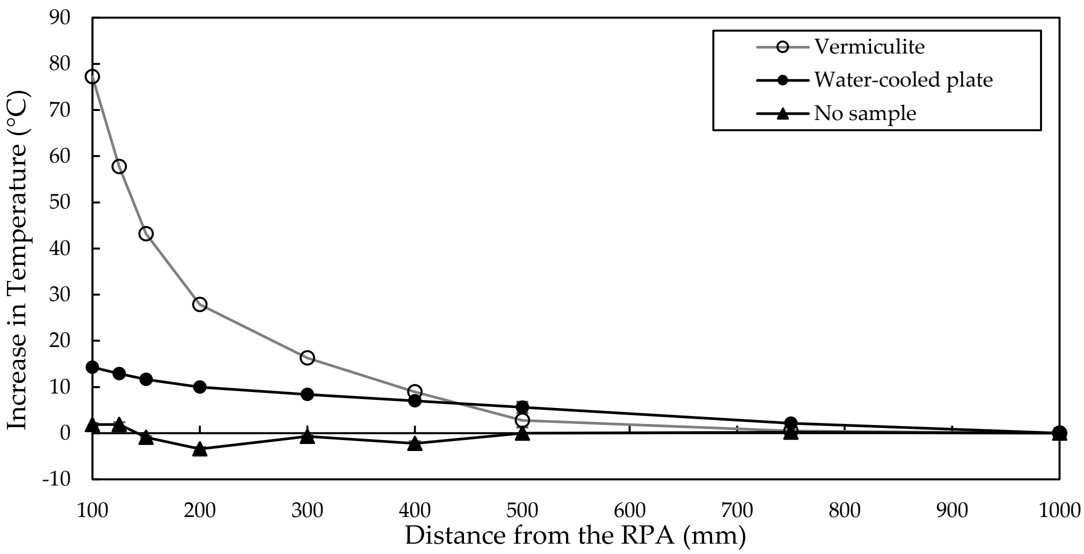

Figure 8 Increase in the surface temperature of the RPA as a function of the separation distance for different cases

As mentioned earlier, the difference between the measured HF when a water-cooled plate was used, and when the HF gauge was used in isolation was 17 % (for a separation distance of 100 mm). This can be clearly seen in Figure 9; the lack of a significantly heated target surface (i.e., using a water-cooled plate) leads to a sizeable reduction in the value of the measured incident HF compared to the case of vermiculite or concrete target samples. The slight increase in the surface temperature of the water-cooled sample, coupled with the presence of the vermiculite shield, led to a small increase of the RPA's surface temperature, which then led to the increase in the value of the HF shown in Figure 9.

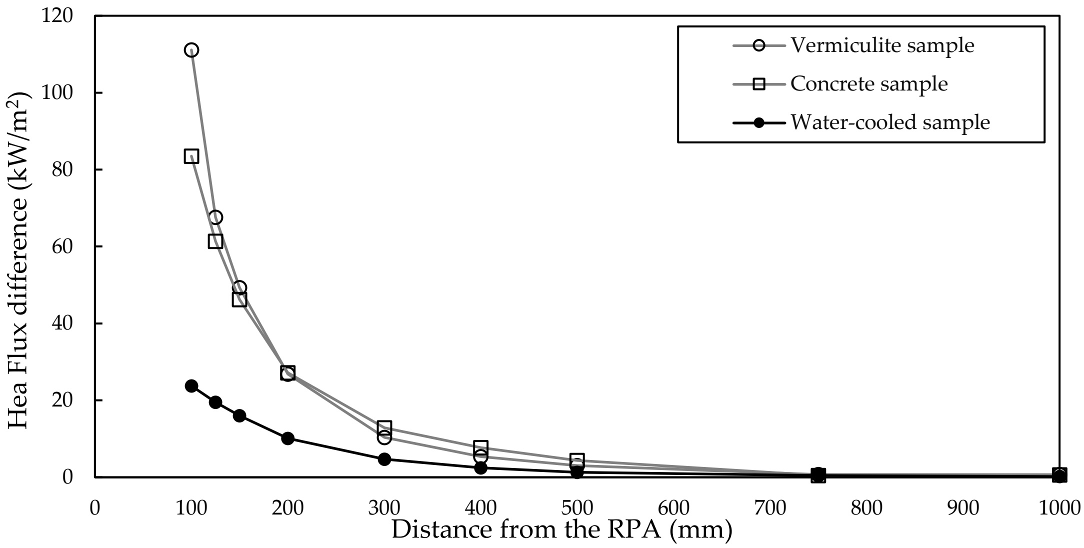

Figure 9 The measured difference of incident HF (as a function of the separation distance) between the no sample case and the water-cooled sample, vermiculite sample, and the concrete sample.

During the experiments, the surface temperature of the water-cooled plate was measured using two TCs that were welded to the surface of the plate. Figure 10 shows the steady-state temperature of the surface of the plate as the separation distance decreased. The surface temperature of the plate reached temperatures as high as 178 °C at the separation distance of 100 mm even with water cooling.

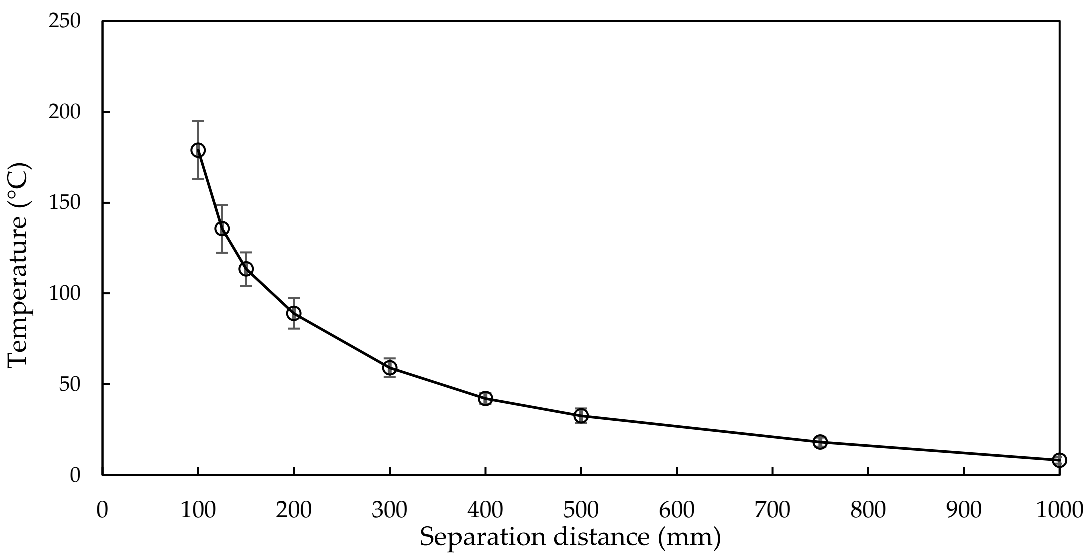

Figure 10 Increase in surface temperature of the water-cooled plate

3.4. Analysis

The increased HF shown in the previous sections is the results of two factors:

1- The influence of the convective zone of the RPA which extends for about 200 mm from the surface of the RPA (see Figure 4).

2- The radiant heat feedback to the RPA from the surface of the heated target samples.

Measurements taken confirmed that the magnitude of the incident HF for the water-cooled plate was greater than that measured with the HF gauge in isolation, but lower than the values recorded using concrete or vermiculite samples (see Figure 9).

3.4.1. The effect of the convection zone and the thermal feedback

To decouple the effects of the zone of convective influence from the effects of the radiant heat feedback, the analysis below can be conducted under the following assumptions. First, the total HF received by the HF gauge can be defined as:

$$\dot{q}^{"}_{inc} = \phi\varepsilon\sigma(T^4_{RPA} - T^4_{HFgauge}) + \dot{q}^{"}_{conv} \quad (2)$$

Where $\dot{q}^{"}_{inc}$ is the incident heat flux, ϕ is the view factor, ε is the emissivity, σ is the Stefan Boltzmann constant, T_{RPA} is the surface temperature of the RPA (in Kelvin), and $\dot{q}^{"}_{conv}$ represents the portion of the heat transfer taking place through convection.

Since the surface temperature of the HF gauge is low due to water cooling, the contribution of $T^4_{HFgauge}$ in the first portion of equation 2 can be omitted. If the temperature and emissivity of the RPA remain constant, as assumed, and the measured incident HF is solely due to radiation (excluding $\dot{q}^{"}_{conv}$ in Equation (2)), $(\dot{q}^{"}_{inc}/\phi)$ can be plotted as a horizontal line against the separation distance. Figure 11 shows this for the cases examined in this study.

Regarding the No Sample case, Figure 11 shows the value of $(\dot{q}^{"}_{inc}/\phi)$ deviates from the reference line as the separating distance becomes smaller, indicating a change either in Emissivity, surface temperature, or contribution from convection. Given that there was no measurable change in the surface temperature (see Figure 8), and with the emissivity assumed to remain constant, all of the rise shown in Figure 11 can be attributed to convective influences. For the No Sample case, the deviation in the value of $(\dot{q}^{"}_{inc}/\phi)$ from the reference line appears to go beyond the 200 mm that was defined as the extent of the convection zone of the RPA (see Figure 4); this may be attributed to uncertainties inherent in the measurement methods, such as view factor calculations, convective effects from ambient air, and other factors. In fact, the increase in $(\dot{q}^{"}_{inc}/\phi)$ beyond a separation distance between 500 and 200 mm is minimal (less than 10% for the no sample case at 300 mm).

For the other cases, the higher values of $(\dot{q}^{"}_{inc}/\phi)$ appear to be the result of heat feedback to the RPA, primarily from the heated samples and some additional contribution from the vermiculite shield (as indicated in Figure 11). In the case of the water-cooled sample, the increased value of $(\dot{q}^{"}_{inc}/\phi)$ stems from both convection and heat feedback from the vermiculite shield. Figure 11 also illustrates a similar trend amongst all cases when the separation distance is large (between 1000 mm and 300 mm). However, as the separation distance drops below 300 mm, divergence becomes evident between cases involving heated samples (concrete or vermiculite) and cases with no sample or a water-cooled sample. While all cases show an upward trend, indicating a higher incident heat flux, the cases with concrete and vermiculite samples show a more significant increase compared to the other cases; this is attributed to feedback from the surface of the heated samples.

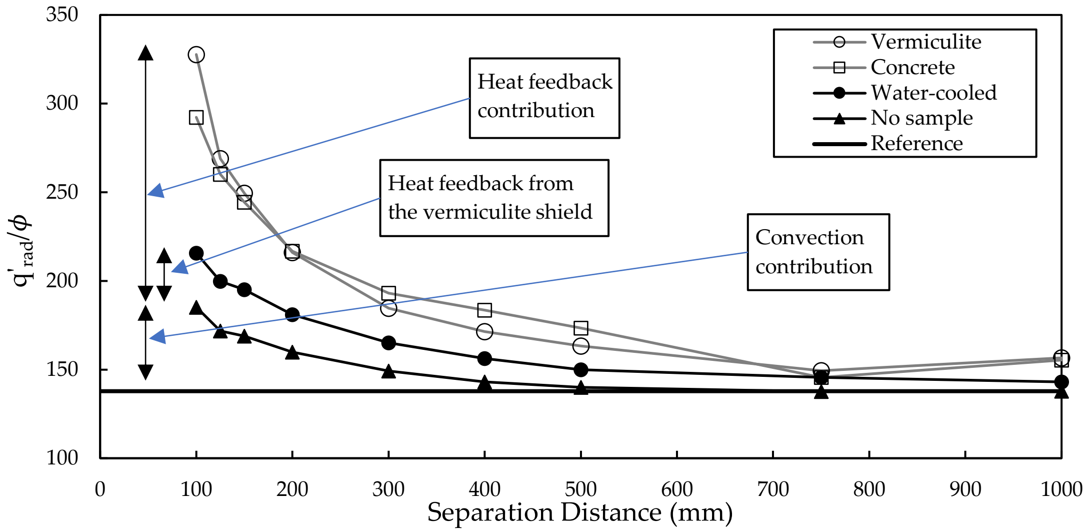

Figure 11 The measured incident HF ($\dot{q}''_{inc}$) divided by the view factor (ϕ) at each separation distance.

Based on the measured values of the incident heat fluxes for each case, the expected surface temperature of RPA can be also approximated, if the other factors shown in Equation (2) are assumed as constants, and omitting the convective portion of Equation (2). By doing this, equating the temperature values demonstrates what the surface temperature of the RPA *would* have been if all the extra HF was coming from radiation alone. Thus, the expected surface temperature of the RPA (for a given separation distance) can be calculated from:

$$T_{RPA} = \sqrt[4]{\frac{\dot{q}''_{inc}}{\phi\varepsilon\sigma}} \tag{3}$$

The difference in the calculated increased surface temperature of the RPA for the vermiculite and the water-cooled samples, compared to the (directly) measured values, has been shown in Figure 12. For the case of no sample, the expected surface temperature of the RPA is rising, even though direct measurements of temperatures showed no such rise. However, it can be noticed that the rise in the computed expected temperatures for the no sample case are almost negligible until the separation distance is 300 mm or less. Further, it was observed that the measured value of the increase in the surface temperature of the RPA for the water-cooled sample was less than the calculated values. This confirms that the increased HF in the cases of water-cooled plate and no sample came mainly from the effects of the zone of convective influence (with some contribution from the heat feedback from the vermiculite shield for the water-cooled plate). Figure 12 also shows that heat feedback from the heated samples drive up the surface temperature of the RPA once the separation distance is about 300 mm or less, and are less important for the surface temperature of the RPA for larger separation distances (for this particular RPA and sample configuration).

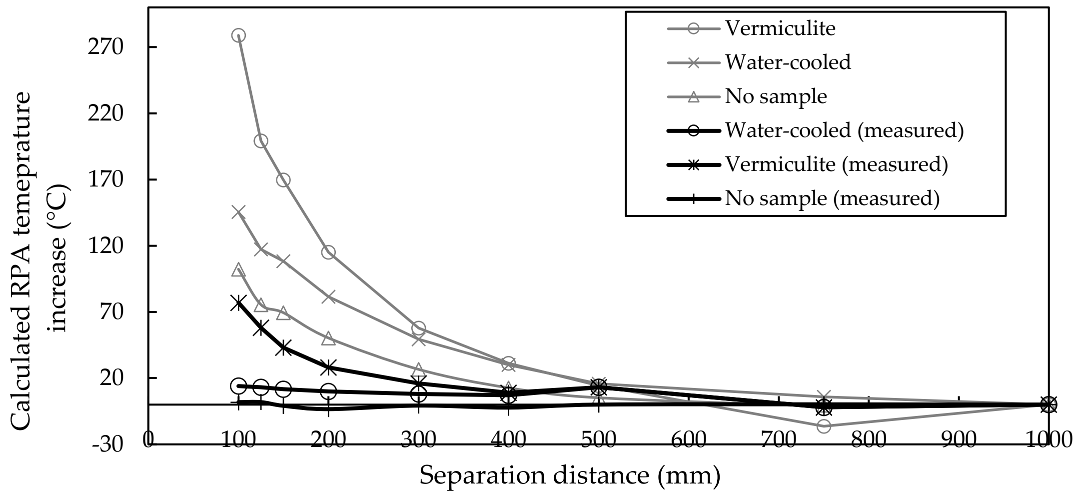

Figure 12 The increase in the surface temperature as calculated from Equation (3), and the direct measurements obtained from experiments.

3.4.2. Quantifying the effects of the thermal feedback

Given that the measured increase in the surface temperature of the RPA is dependent on the target sample, it is possible to show the "additional" measured HF as function of the measured increase in the RPA surface temperature for the vermiculite and the water-cooled sample. The radiant incident HF for each case can be written as:

$$\dot{q}''_{rad\ (WC)} = \phi\varepsilon\sigma T^4_{RPA,WC} \tag{4}$$

$$\dot{q}''_{rad\ (V)} = \phi\varepsilon\sigma T^4_{RPA,V} \tag{5}$$

Where $\dot{q}''_{rad\ (WC)}$ is the radiant HF when a water-cooled plate is used, and $\dot{q}''_{rad\ (V)}$ is when a Vermiculite sample is used. When considering the two experimental conditions (i.e., vermiculite and water-cooled plate), the view factor for any given separation distance remains constant. While the emissivity of the RPA may change slightly as a function of temperature, the variation is assumed negligible over the range of temperature differences used in this analysis. This leaves the irradiance of the panel to be dependent on the magnitude of T^4_{RPA}.

The increase in the incident HF when using a vermiculite sample can thus be written as:

$$Heat\ flux\ increase = \Delta\dot{q}''_{rad} = \dot{q}''_{rad\ (V)} - \dot{q}''_{rad\ (WC)} \tag{6}$$

And having noted previously that the view factor and emissivity are assumed constant (for any given separation distance), the increase in HF would be:

$$\Delta\dot{q}''_{rad} = \phi\varepsilon\sigma T^4_{RPA(V)} - \phi\varepsilon\sigma T^4_{RPA(WC)} \tag{7}$$

Equation 7 can be simply written as:

$$\Delta\dot{q}''_{rad} \propto \phi(T^4_{RPA(V)} - T^4_{RPA(WC)}) \tag{8}$$

Figures 13 and 14 show the result of this exercise; the increase in the measured HF is directly proportional to the increase in the surface temperature raised to the fourth power.

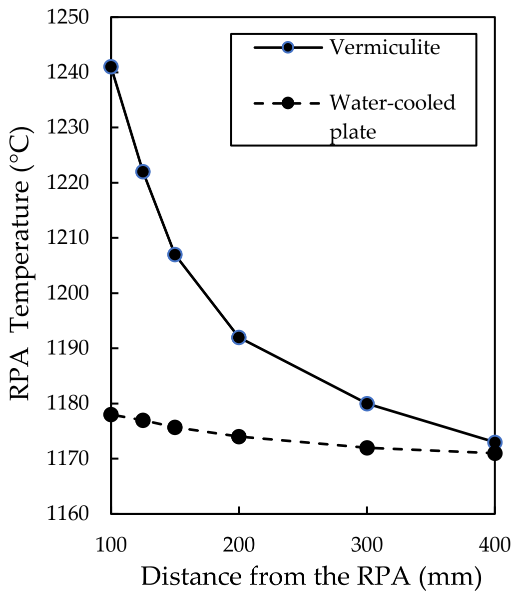

Figure 13 comparison between surface temperature of the RPA for a vermiculite sample and a water-cooled plate.

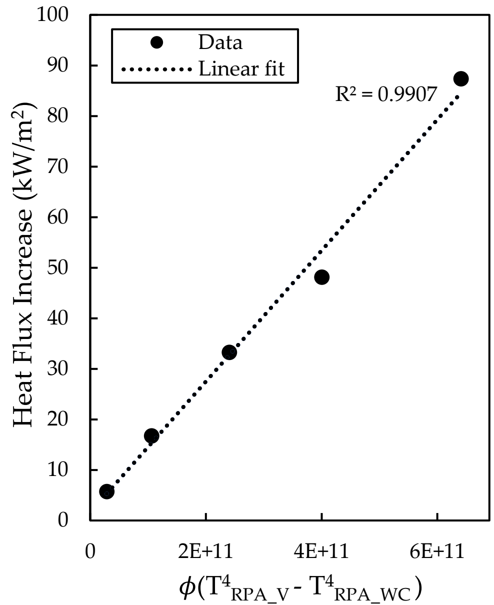

Figure 14 The relationship between the increase in the measured HF and the increase in the surface temperature of the RPA (in degrees Kelvin).

Figure 14 shows that there is a linear relationship between the increase in the surface temperature of the RPA (to the fourth power) and the measured HF increase. Therefore, an RPA user can measure the increase in the surface temperature of the RPA to obtain the increased HF that would not be accounted for in a traditional calibration (i.e., by using a HF gauge in isolation).

The increase in HF values illustrated in this work are a potential concern for those using RPA in research applications, and ought to be taken into account. To measure the increased heat flux, it may not be practical to embed HF gauges into test samples (as seen in this study) in all applications. Therefore, this correlation allows experimentalist to account for calibration errors and increases in HF boundary conditions that result from thermal feedback during an experiment. The authors therefore encourage RPA users to monitor the temperatures of the RPA over the duration of their experiments; if any increase in temperature is observed, this can at least be accounted for when considering further analysis using the boundary conditions provided by the RPA. The data shown in Figure 14 also suggest that users can employ control system techniques to regulate the calibrated HF to target samples. If the RPA temperature is continuously monitored, then a simple PID system could adjust the panel positions to account for both the calibrated HF at a target location (assuming a constant panel temperature) and the increase in HF from the elevated RPA temperature. This would be similar to the principle used in the Cone Calorimeter, except in this case the variable would be the position of the RPA (relative to the target sample) as opposed to the power supply to the Cone.

4. CONCLUSIONS

This paper has identified and quantified the effects of the thermal feedback from a target sample on the thermal boundary conditions when using a gas-fired RPA in fire testing. While other testing apparatus such as the cone calorimeter have mechanisms to maintain the surface temperature of the cone constant during experiments, no such capability currently exists for most gas-fired RPAs.

To investigate this, and using a mobile RPA at the University of Edinburgh [3], [14], [15], incident heat fluxes at various separation distances were measured under a range of conditions. Experiments were repeated for varying set-ups, namely: the HF gauge in isolation, the HF gauge embedded in a vermiculite sample, the HF gauge embedded in a concrete sample, and the HF gauge embedded in a water-cooled aluminium plate. From the results, the following conclusions can be drawn:

1. The increase in the surface temperature of a target sample may significantly affect the thermal boundary conditions provided by a gas-fired RPA. This effect is manifested in an increase in the surface temperature of the RPA, and, consequently, the heat flux imposed on the target sample. In this study, the incident heat flux to the heated target sample increased as much as 78% from the calibrated value due to thermal feedback.

2. It was confirmed that the presence of a Vermiculite sample led to an increase of almost 80 °C (at a separation distance of 100 mm) in the surface temperature of the RPA. By comparison, the surface temperature of the RPA increased by only 14 °C only (for the same separation distance) when a water-cooled plate was used in-lieu of a vermiculite sample. The small rise in the surface temperature of the RPA for the case of the water-cooled plate appeared to originate from the heat feedback from the vermiculite shield used to protect the instrumentation from exposure to heat.

3. The zone of convective influence was confirmed to significantly impact on the value of the measured incident heat flux; however, this effect could be accounted for should the users of an RPA utilise a water-cooled heat flux gauge to calibrate the RPA. The extent of this zone (for the particular RPA used in this study) is approximately 200 mm from the surface of the RPA.

4. The relationship between the increase in the measured heat flux and the surface temperature of the RPA (raised to the fourth power) is – as expected – linear. This enables the temperature increase to be corrected for in future experimentation, while the effects of the zone of convective influence can be accounted for by using a heat flux gauge.

5. The increase in the surface temperature of the RPA is considered important to properly characterise the boundary conditions imposed on a specimen when using a pre-calibrated gas-fired RPA. Monitoring the surface temperature of RPAs is thus important during RPA experiments, so that users can correct for the incident heat fluxes; by using the correction method offered above or by altering the RPA to account for the rise in its surface temperature and adjust its position accordingly in real time.

6. VALUES determined in the study might not be directly applicable to other systems, but the general observations and most importantly the logic behind your correction method are applicable to any system – and these effects need to be considered by all RPA users.

REFERENCES

[1] "BSI Standards Publication ISO 5660-2:3025. Reaction-to-fire tests — Heat release, smoke production and mass loss rate," vol. 3rd, no. January, p. 64, 2019.

[2] ASTM, “Standard Test Methods for Measurement of Synthetic Polymer Material Flammability Using a Fire Propagation Apparatus (FPA),” *Des. E2058 − 19*, vol. i, pp. 1–29, 2019, doi: 10.1520/E2058-19.2.

[3] C. Maluk, L. Bisby, M. Krajcovic, and J. L. Torero, “A Heat-Transfer Rate Inducing System (H-TRIS)Test Method,” *Fire Saf. J.*, vol. 105, pp. 307–319, 2019, doi: 10.1016/j.firesaf.2016.05.001.

[4] T. Hulin, C. Maluk, L. Bisby, K. Hodicky, J. W. Schmidt, and H. Stang, “Experimental Studies on the Fire Behaviour of High Performance Concrete Thin Plates,” *Fire Technol.*, vol. 52, no. 3, pp. 683–705, 2016, doi: 10.1007/s10694-015-0486-x.

[5] C. Maluk, L. Bisby, G. Terrasi, and M. Green, “Bond strength of CFRP and steel bars in concrete at elevated temperature,” *Am. Concr. Institute, ACI Spec. Publ.*, no. 279 SP, pp. 41–75, 2011, doi: 10.14359/51682965.

[6] A. Elliott, A. Temple, C. Maluk, and L. Bisby, “Novel testing to study the performance of intumescent coatings under non-standard heating regimes,” *Fire Saf. Sci.*, vol. 11, pp. 652–665, 2014, doi: 10.3801/IAFSS.FSS.11-652.

[7] C. Maluk, L. Bisby, and G. P. Terrasi, “Effects of polypropylene fibre type and dose on the propensity for heat-induced concrete spalling,” *Eng. Struct.*, vol. 141, pp. 584–595, 2017, doi: 10.1016/j.engstruct.2017.03.058.

[8] I. Rickard, M. Spearpoint, and S. Lay, “The performance of laminated glass subjected to constant heat fluxes related to building fires,” *Fire Mater.*, no. October 2020, pp. 283–295, 2020, doi: 10.1002/fam.2939.

[9] A. I. Bartlett, R. M. Hadden, L. A. Bisby, and A. Law, “Analysis of cross-laminated timber charring rates upon exposure to nonstandard heating conditions,” *Fire Mater. 2015 - 14th Int. Conf. Exhib. Proc.*, no. August, pp. 667–681, 2015.

[10] A. Cicione, K. Mazolwana, J. Kruger, R. Walls, Z. Sander, and G. Van Zijl, “Effect of transverse and longitudinal confinement on the interlayer bond in 3D printed concrete at elevated temperatures: an experimental study,” pp. 184–195, 2020, doi: 10.14264/d006b39.

[11] A. Cicione, J. Kruger, R. S. Walls, and G. Van Zijl, “An experimental study of the behavior of 3D printed concrete at elevated temperatures,” *Fire Saf. J.*, vol. 120, no. April 2020, p. 103075, 2021, doi: 10.1016/j.firesaf.2020.103075.

[12] H. Mohammed, F. Sultangaliyeva, M. Wyrzykowski, G. Pietro Terrasi, and L. A. Bisby, “An Experimental Study into the Behaviour of Self-Prestressing, Self-Compacting Concrete at Elevated Temperatures,” in *7th International Workshop on Concrete Spalling due to Fire Exposure, 12-14 October 2022*, 2022, pp. 179–193, [Online]. Available: https://nbn-resolving.org/urn:nbn:de:kobv:b43-560798.

[13] H. Mohammed, F. Sultangaliyeva, M. Wyrzykowski, G. Pietro Terrasi, and L. Bisby, “Heat-induced explosive spalling of self-prestressing, self-compacting concrete slabs,” *Constr. Build. Mater.*, vol. 372, no. February, p. 130821, 2023, doi: 10.1016/j.conbuildmat.2023.130821.

[14] H. Mohammed, D. Morrisset, A. Law, and L. Bisby, "Quantification of the thermal environment surrounding radiant panel arrays used in fire experiments," in *12th Asia-Oceania Symposium on Fire Science and Technology (AOSFST 2021*, 2021, no. December, pp. 7–9, doi: 10.14264/6efaa82.

[15] I. Rickard, "Explosive Spalling of Concrete in Fire: Novel Experiments under Controlled Thermal and Mechanical Conditions," p. 390, 2020, [Online]. Available: https://era.ed.ac.uk/handle/1842/37473.

[16] D. Drysdale, *An Introduction to Fire Dynamics: Third Edition*. 2011.

[17] Tobias Laschützа, "Numerical and experimental investigation of a Thin Skin Calorimeter (TSC)," The University Of Edinburgh, 2017.

[18] V. Babrauskas, "Development of the cone calorimeter—A bench-scale heat release rate apparatus based on oxygen consumption," *Fire Mater.*, vol. 8, no. 2, 1984, doi: 10.1002/fam.810080206.

[19] AFNOR, "NF EN 1992-1-2 / NA Eurocode 2 : Calcul des structures en béton — Partie 1-2 : Règles générales — Calcul du comportement au feu - Annexe Nationale a la NF EN 1992-1-2:2005 - Calcul du comportement au feu," vol. 2, no. Octobre 2007, p. 30, 2007.

[20] *SFPE Handbook of Fire Protection Engineering*, 5th ed. 2016.